

Quantum-mechanical wavepacket transport in quantum cascade laser structures

S.-C. Lee,¹ F. Banit,¹ M. Woerner,² and A. Wacker^{3,*}

¹*Institut für Theoretische Physik, Technische Universität Berlin, 10623 Berlin, Germany*

²*Max-Born-Institut für Nichtlineare Optik und Kurzzeitspektroskopie, 12489 Berlin, Germany*

³*Fysiska Institutionen, Lunds Universitet, Box 118, 22100 Lund, Sweden*

(Dated: to appear in Physical Review B 2006)

We present a viewpoint of the transport process in quantum cascade laser structures in which spatial transport of charge through the structure is a property of coherent quantum-mechanical wavefunctions. In contrast, scattering processes redistribute particles in energy and momentum but do not directly cause spatial motion of charge.

I. INTRODUCTION

Unipolar quantum cascade (QC) laser devices¹ are intraband semiconductor devices in which the transport processes and optical (intersubband) transitions which give rise to the lasing operation occur only in the conduction band of the semiconductor structure. This marks a departure from previous interband semiconductor lasers. Since the first realization of a QC laser, there has been a proliferation of QC laser designs.² QC laser structures are composed of a complicated sequence of semiconductor layers with different material compositions and thicknesses. This sequence is repeated tens or hundreds of times giving rise to a periodic structure in the device. Considering the complicated layer composition of these devices, the nature of the charge transport process through these structures is not immediately apparent.

The original concept by Kazarinov and Suris³ was based on coherent tunneling between neighboring wells. It was soon realized however that scattering plays a crucial role in establishing the nonequilibrium carrier distribution, in particular for the depopulation of the lower laser level. Thus almost all simulations of transport^{4,5,6,7} in QC structures assume a semiclassical model, in which the transport occurs through scattering transitions between energy eigenstates (Wannier-Stark hopping⁸). In such an approach only diagonal elements of the density matrix (populations or distribution functions) in the Wannier-Stark basis are used, and offdiagonal elements are neglected (hence, the term semiclassical). Ref. 5 briefly considered a more fully quantum-mechanical extension to this semiclassical approach by also including offdiagonal elements (coherences) of the density matrix in the calculation. This study concluded that quantum-mechanical coherences were of limited importance to the transport properties. However, coherent effects were observed experimentally for the electron transfer from the injector to the upper laser level in QC structures.^{9,10} The importance of coherent effects has also recently been stressed by Ref. 11, where a simplified calculation scheme is proposed.

The concept that scattering transitions propel the current through heterostructure systems conflicts with the standard description of transport in bulk structures, where complex Bloch functions carry the current, while

scattering redistributes the carriers in momentum space but does not change their spatial positions.¹² We will show that a similar description also holds in quantum cascade lasers where the current is carried by quantum-mechanical wavepackets, and the scattering only acts locally redistributing carriers in energy or momentum.

II. THE MODEL

The quantum-mechanical transport theory we use here is based on nonequilibrium Green's functions which allow for a consistent combination of scattering and coherent evolution. Quantum-mechanical coherences are represented by offdiagonal elements of the $G^<(E)$ correlation function, which is related to the density matrix $\rho_{\alpha\mathbf{k},\beta\mathbf{k}} = \int dE G_{\alpha\beta,\mathbf{k}}^<(E)/2\pi i$. The theory is formulated with basis states $\Psi_{\alpha\mathbf{k}}(\mathbf{r}, z) = (e^{i\mathbf{k}\cdot\mathbf{r}}/\sqrt{\mathcal{A}})\psi_{\alpha}(z)$. Here $\psi_{\alpha}(z)$ is the envelope function in the growth direction z . The wavevector \mathbf{k} and the spatial coordinate \mathbf{r} are two-dimensional vectors in the plane of each semiconductor layer (with normalization area \mathcal{A}), taking fully into account the three-dimensional nature of the structure.

We divide the total Hamiltonian as $\hat{H} = \hat{H}_o + \hat{H}_{\text{scatt}}$. The free Hamiltonian \hat{H}_o contains the kinetic energy and applied voltage, together with the electron-electron interaction in a mean field approximation. It is diagonal in \mathbf{k} , while \hat{H}_{scatt} describes scattering interactions $\mathbf{k} \rightarrow \mathbf{k}'$. Here we explicitly take into account acoustic phonon and longitudinal optical phonon, impurity, and interface roughness scattering processes. \hat{H}_{scatt} is treated perturbatively using self-energies in the self-consistent Born approximation. For example, for impurity scattering, the self-energy has the form

$$\Sigma_{\alpha\alpha',\mathbf{k}}^{<,\text{imp}}(E) = \sum_{\beta\beta',\mathbf{q}} \langle V_{\alpha\beta}^{\text{imp}}(\mathbf{q}) V_{\beta'\alpha'}^{\text{imp}}(-\mathbf{q}) \rangle G_{\beta\beta',\mathbf{k}-\mathbf{q}}^<(E) \quad (1)$$

where V^{imp} represents the impurity scattering potential.²⁵ In the following, we consider both the complete form of Eq. (1) with nondiagonal self-energies (ND), as well as approximations summarized in Table I. In each case, the system of equations for the Green's functions and self-energies is solved self-consistently, which is an extensive numerical task.²⁶ This results

	$\langle V_{\alpha\alpha} V_{\alpha\alpha} \rangle$	$\langle V_{\alpha\beta} V_{\beta\alpha} \rangle$	$\langle V_{\alpha\alpha} V_{\beta\beta} \rangle$	$\langle V_{\alpha\beta} V_{\beta'\alpha'} \rangle$
DG	•	•	–	–
ND	•	•	•	•
NDL	•	–	•	–

TABLE I: Scattering potential matrix elements included in different self-energy models. • (–) indicates scattering potential matrix elements included (excluded) from the self-energy. The scattering potential V may represent impurity, interface roughness, or phonon scattering. The angle brackets represent an averaging over the impurity distribution for impurity scattering, the distribution of thickness fluctuations for interface roughness scattering, and phonon modes for phonon scattering. DG indicates diagonal self-energies, while ND represents nondiagonal self-energies. NDL restricts the scattering matrix elements to local terms $V_{\alpha\alpha}$ for ND.

in the determination of the full correlation function $G_{\beta\alpha,\mathbf{k}}^<(E)$, which describes the nonequilibrium state of the device.

Current densities are defined as $J = J_o + J_{\text{scatt}}$ with

$$J_o = \frac{ie\langle[\hat{H}_o, \hat{z}]\rangle}{\mathcal{V}\hbar} = \frac{2e}{\hbar\mathcal{V}} \sum_{\alpha\beta,\mathbf{k}} \int \frac{dE}{2\pi} [\hat{H}_o, \hat{z}]_{\alpha\beta} G_{\beta\alpha,\mathbf{k}}^<(E) \quad (2)$$

and $J_{\text{scatt}} = ie\langle[\hat{H}_{\text{scatt}}, \hat{z}]\rangle/\mathcal{V}\hbar$. $e < 0$ is the electron charge and \mathcal{V} is the sample volume. In Ref. 13 it was shown that J_{scatt} provides the hopping current due to scattering transitions between the states if one restricts to diagonal Green functions and self-energies, i.e. neglects coherences between the states. Thus this part was referred to as scattering current, reflecting the (mis-)conception that current flow occurs by a combination of both coherent evolution (J_o) and relocation by scattering transitions. In the following we will show that J_{scatt} vanishes if coherences are properly taken into account, while the entire current is carried by J_o .

Basis states: The basis functions $\psi_\alpha(z)$ can be chosen in different ways. In theory, the choice of basis states should not affect the physical results. In practice, this choice can influence the physical description in several ways: i) approximations are always necessary to perform the theoretical calculation or to facilitate the numerical computation, and the interplay between the chosen basis and the approximations may improve or reduce the validity of the approximations and hence affect the physical result, ii) different choices of basis states can reveal different physical aspects of the problem. For instance, as we show in this paper, working with position eigenstates casts light on spatial aspects of the problem.

In our earlier work,¹³ spatially-localized Wannier states were used as an orthonormal set of $\psi_\alpha(z)$, which can be constructed for the infinitely extended QC structure in a straightforward manner and generate a well-defined periodic Hamiltonian. A second type of states are the Wannier-Stark states, which are the eigenstates of \hat{H}_o . They can be easily obtained by diagonalizing \hat{H}_o in the basis of Wannier states. (This procedure avoids

the common use of an artificial spatial confinement.) A third type of states constitutes the position eigenstate basis, using the eigenfunctions of the position operator \hat{z} . Again we start with the Wannier basis, diagonalize \hat{z} , and transform \hat{H}_o into the new basis. In all bases we evaluate the scattering matrix elements directly for the respective basis functions.

Structures: The data presented below was obtained using two typical examples: (A) a midinfrared QC laser¹⁴ and (B) a THz QC laser.¹⁵ In the calculation we restrict the number of basis functions to 9 (5) per period for structures A (B).

III. VANISHING OF J_{scatt}

In Ref. 13, we neglected the offdiagonal elements of the self-energies, i.e., only terms with $\alpha = \alpha'$ and $\beta = \beta'$ (diagonal self-energy, DG in Table I) were included in Eq. (1). In this restricted theory, we found J_o and J_{scatt} to be similar in magnitude. In contrast, using the more rigorous and complete formulation of the theory reported here, where all self-energy terms are included (nondiagonal self-energies, ND), we find that $J_{\text{scatt}} \approx 0$. This result is basis invariant if the complete nondiagonal self-energies (ND) are used, as we checked this explicitly (numerically) for all three types of basis sets. Hence the total current density is given by J_o .

The same result has recently been analytically demonstrated by Lake and Pandey.¹⁶ In the position eigenstate basis, where the matrix $z_{\alpha\beta}$ is diagonal, the expression (16) for J_{scatt} of Ref. 13 becomes

$$J_{\text{scatt}} = \frac{2e}{\hbar\mathcal{V}} \sum_{\mathbf{k}} \int \frac{dE}{2\pi} \sum_{\alpha\beta} z_{\alpha\alpha} \left(G_{\alpha\beta,\mathbf{k}}^< \Sigma_{\beta\alpha,\mathbf{k}}^{\text{adv}} + G_{\alpha\beta,\mathbf{k}}^{\text{ret}} \Sigma_{\beta\alpha,\mathbf{k}}^< - \Sigma_{\alpha\beta,\mathbf{k}}^< G_{\beta\alpha,\mathbf{k}}^{\text{adv}} - \Sigma_{\alpha\beta,\mathbf{k}}^{\text{ret}} G_{\beta\alpha,\mathbf{k}}^< \right)$$

Now the term in brackets corresponds to the right-hand side of the continuity equation as given in Eq. (57) of Ref. 17, which has to vanish. See also Section 2.4 of Ref. 18.

A second line of argument runs as follows: For microscopic scattering potentials which only depend on $\hat{\mathbf{r}}$ (but not on momentum \hat{p}), the commutator $[\hat{H}_{\text{scatt}}, \hat{z}]$ vanishes and hence $J_{\text{scatt}} = 0$ by its definition. Thus $J_{\text{scatt}} = 0$ holds for a wider class of scattering processes, including electron-electron scattering, than studied numerically here. These analytic arguments demonstrate that the previous observation of a finite J_{scatt} in Ref. 13 is an unphysical result caused by the DG-approximation in the self-energies for a nonlocal basis of Wannier functions.

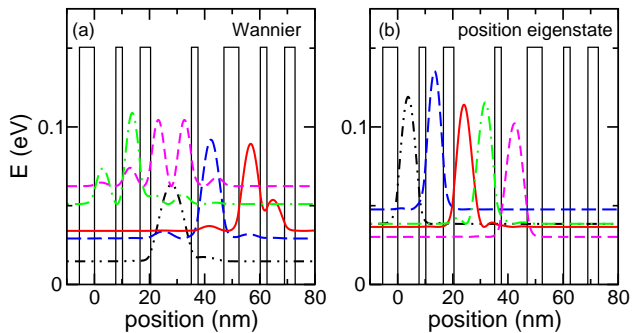


FIG. 1: (Color online.) Wavefunctions (modulus-squared) for Structure B. (a) Wannier, (b) Position eigenstates.

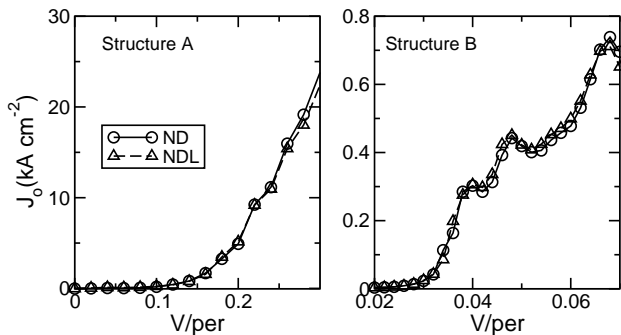


FIG. 2: Current-voltage characteristic in position eigenstate basis with self-energy models ND and NDL. We display J_0 ; $J_{\text{scatt}} \approx 0$ in both cases.

IV. SPATIALLY-LOCAL SCATTERING IN J_o

Although J_{scatt} vanishes this does not imply that scattering processes are absent from the transport process. These processes do not appear explicitly in Eq. (2) but they act implicitly in determining $\mathbf{G}^<(E)$, and hence in driving the current J_o . We now investigate the role played by scattering processes in determining J_o . In particular, we seek to establish if each scattering event results in a spatial displacement of charge, or if a scattering process acts locally resulting in energy redistribution but with no accompanying spatial transport.

This issue can be conveniently addressed within the basis of position eigenstates. In contrast to the Wannier wavefunctions [Fig. 1(a)], these position eigenfunctions are localized to within a single well layer in the structure [see Fig. 1(b)] and the scattering potential matrix elements $\langle \alpha | V | \beta \rangle$ are significantly smaller for $\alpha \neq \beta$ than for $\alpha = \beta$. We therefore compare the effect of excluding or including certain scattering potential terms in the self-energies, see Table I.

Fig. 2 shows that J_o^{NDL} and J_o^{ND} are almost identical for both samples. This indicates that the potential terms $\langle V_{\alpha\alpha} V_{\alpha\alpha} \rangle$ and $\langle V_{\alpha\alpha} V_{\beta\beta} \rangle$ constitute the main contribution to the self-energies in the calculation of J_o^{ND} , our most rigorous formulation of the current. These scattering terms involve only purely local (in space) transi-

tions, as $V_{\alpha\alpha}$ represents a transition matrix element between states with the same envelope function $\psi_\alpha(z)$, i.e., localized to the same well. This implies that the scattering processes act only locally in space. They do not cause spatial displacement of charge, but act only to redistribute momentum \mathbf{k} and energy.

A key point of our argument was the use of the position eigenstate basis which enabled us to demonstrate that the dominant scattering processes in J_o act locally and therefore do not contribute to the spatial transport of charge by J_o . This result is not evident if we work in another basis, e.g., Wannier or Wannier-Stark, where the wavefunctions are far more delocalized and off-diagonal matrix elements $V_{\alpha\beta}$ play a significant role. Nevertheless, physical mechanisms, such as the nature of transport, must be basis invariant. Indeed, as long as the full self-energies are taken into account, the expression for the currents J_0 and J_{scatt} are invariant under basis transformations. This demonstrates that the same result is recovered even in the case of a delocalized basis, where the interplay of all types of matrix elements in Table I reproduces the locality of scattering transitions. In contrast, the neglect of certain matrix element combinations (such as the DG-approximation) generates spurious non-local scattering transition in a delocalized basis.

V. TRANSPORT OF J_o BY COHERENT WAVE FUNCTIONS

As we have just seen, the scattering processes which contribute to J_o have a purely local effect which does not spatially displace carriers. Hence, we conclude that the transport of charge by J_o through the structure must arise as a property of the quantum-mechanical wavefunction. We can obtain a more concrete visualization of this transport mechanism by resolving J_o in energy and space:

$$J_o(E, z) = \frac{e}{\pi \mathcal{A}} \sum_{\alpha\beta, \mathbf{k}} \text{Re} \left\{ \frac{-\hbar}{m(z)} \psi_\alpha^*(z) \frac{\partial \psi_\beta(z)}{\partial z} G_{\beta\alpha, \mathbf{k}}^<(E) \right\}. \quad (3)$$

The lower panel of Fig. 3 show that the current $J_o(E, z)$ flows at different energies in different spatial regions of the structures. To satisfy the equation of continuity, scattering interactions enable energy transitions which occur locally as discussed above (an example is depicted by the vertical arrow in the figure). Thus, scattering gives rise to a redistribution of electrons in energy but does not cause a spatial displacement or spatial transport of charge.²⁷

Fig. 4 shows the corresponding result for sample A. Here the current density is restricted to a narrow energy range while crossing the thick barrier (around $z = -2$ nm) between the injector and the active region, thus providing the desired selective feeding of the upper laser level. This demonstrates how this representation allows for a detailed insight into the microscopic operation of

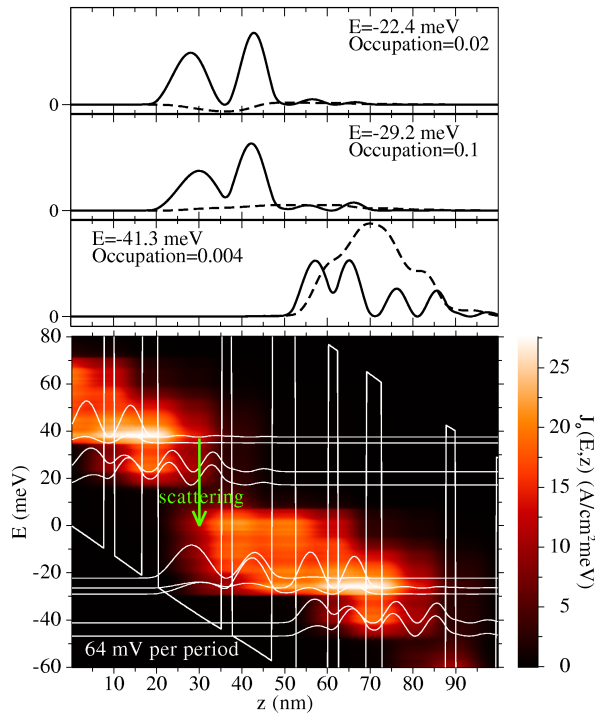


FIG. 3: (Color online.) *Lower panel:* Spatially and energetically resolved current from Eq. (3) for sample B. The wavefunctions depict some quasi-levels, which are eigenstates of \hat{H}_o at $\mathbf{k} = 0$ renormalized by the scattering interactions. *Upper panels:* Probability density $|\phi_{n\mathbf{k}}(z)|^2$ (black line) and current $\propto \text{Re}\{-i\phi_{n\mathbf{k}}^* \phi'_{n\mathbf{k}}(z)/m(z)\}$ (dashed line) for the complex wave functions $\phi_{n\mathbf{k}}(z)$ for $\mathbf{k} = 0$. n corresponds to the largest eigenvalue $f_{n0}(E)$ for the respective values of E . These energies are chosen as local maxima E_{max} of $f_{n0}(E)$ with FWHM ΔE (~ 1 meV) and the respective occupations have been approximated by $(\pi/2)f_{n0}(E_{\text{max}})\Delta E$.

the device.

An especially intuitive form of Eq. (3) can be obtained by transforming into an (energy-dependent) basis of eigenstates of the hermitian matrix $-i/(2\pi)G_{\beta\alpha, \mathbf{k}}^{\leq}(E)$ which has real eigenvalues $f_{n\mathbf{k}}(E)$. While $f_{n\mathbf{k}}(E)$ exhibits sharp peaks in energy, the eigenstates $\phi_{n\mathbf{k}}(z)$ exhibit only a weak energy dependence (not shown for brevity). Then we find

$$J_o(E, z) = \frac{2e}{\mathcal{A}} \sum_{n\mathbf{k}} f_{n\mathbf{k}}(E) \text{Re} \left\{ \phi_{n\mathbf{k}}^*(z) \frac{(-i\hbar)}{m(z)} \frac{\partial \phi_{n\mathbf{k}}(z)}{\partial z} \right\}. \quad (4)$$

Thus, the energy-resolved current is carried by wave functions $\phi_{n\mathbf{k}}(z)$ with occupation densities $f_{n\mathbf{k}}(E)$ (the factor 2 is due to spin). This is analogous to the Bloch functions and their occupation in standard bulk transport. The upper panels of Fig. 3 show that these current carrying states $\phi_{n\mathbf{k}}(z)$ extend over a range of one period. This length scale gives a measure of the coherence length, i.e., the distance over which charge is transported by a single coherent wave packet. The peaks in density $|\phi_{n\mathbf{k}}(z)|^2$ are localized in the wells as charge tends to accumulate in the

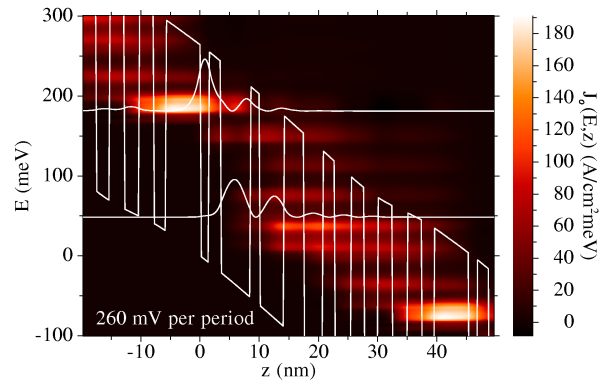


FIG. 4: (Color online.) Spatially and energetically resolved current from Eq. (3) for sample A. The quasi-levels, which are eigenstates of \hat{H}_o at $\mathbf{k} = 0$ renormalized by the scattering interactions are shown for the upper and lower laser state for comparison.

low-potential regions. The currents carried by the wave functions $\phi_{n\mathbf{k}}(z)$ are more evenly distributed which reflects the ability of the wave packets to transport charge across the structure. Note the nonvanishing divergence of current density which reflects the local balance of scattering processes. Thus, these complex wave functions $\phi_{n\mathbf{k}}(z)$ can be viewed as generalized states for a nonequilibrium system, where the drive by bias and scattering processes compensate.

The currents associated with these wavepackets can differ significantly: The state at -29.2 meV (corresponding to the upper laser level) has only a small current, but a high occupation. In contrast, the state at $E = -41.3$ meV (lower laser level) exhibits a strong current to the right, effectively moving electrons away from the lasing transition which occurs vertically between these states. There are also states exhibiting local current flow to the left, e.g., at -22.4 meV. Such considerations may provide new tools for the optimization and design of new laser structures.

The complex states $\phi_{n\mathbf{k}}(z)$ are of particular importance at level crossings. This is demonstrated in Fig. 5 for a simple superlattice at the resonance between the ground state and the first excited state of the neighboring well. Fig. 5(a) depicts the Wannier-Stark states, which are spread over both wells. The first two eigenvalues $f_{n0}(E)$ (for $\mathbf{k} = 0$) exhibit a clear peak at the level energies [see Fig. 5(b)] and the corresponding states, carry particles to the right [state 1, Fig. 5(c)] and to the left [state 2, Fig. 5(d)]. However, the occupation of the state 1 is about two orders of magnitude larger thus providing a strong current flux over the barrier.

Our viewpoint of current-carrying coherent wavefunctions differs essentially from the conception that scattering transitions propel the current. This manifests itself in two ways: (i) In a scattering transition picture, the current would stop immediately once the scattering processes stop (H_{scatt} drops to zero). However, the oc-

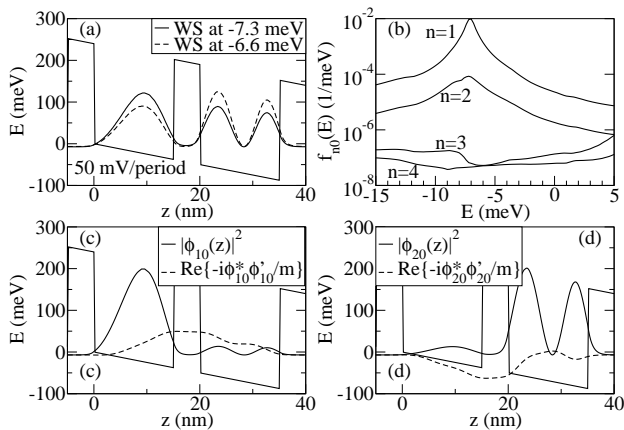


FIG. 5: States for the superlattice of Ref. 19. (a) Doublet of Wannier-Stark states. (b) Eigenvalues $f_{n\mathbf{k}}(E)$ of $-i/(2\pi)G_{\beta\alpha,\mathbf{k}}^< (E)$ for $\mathbf{k} = 0$. (c,d) Corresponding eigenfunctions $\phi_{n\mathbf{k}}(z)$ at $E = -7\text{meV}$, for the two largest eigenvalues, $f_{1\mathbf{k}}$ and $f_{2\mathbf{k}}$, respectively.

cupation of current-carrying wave-functions only changes on the scale of the scattering time, thus the current flow will continue on this time scale. (ii) The current is sensitive to quantum mechanical phases. E.g., phase conjugation would reverse the direction of J_o , while scattering rates would be unaffected.

VI. RELATION TO WANNIER-STARK HOPPING MODEL

In the Wannier-Stark hopping model, the current is carried by scattering transitions between Wannier-Stark states and depends only on scattering rates and the populations of these states. The coherences, i.e., offdiagonal elements $\rho_{\alpha\mathbf{k},\beta\mathbf{k}}$ (diagonal in \mathbf{k} in contrast to scattering transition amplitudes $\rho_{\alpha\mathbf{k},\beta\mathbf{k}'}$) of the density matrix, play no role in this model and are neglected. There are two peculiarities in this picture: (i) The Wannier-Stark hopping picture of transport through scattering transitions and our picture of transport by coherent wavepackets each provide the entire current and yet offer such conflicting views of the transport mechanism. (ii) If we examine Eq. (2) expressed in the Wannier-Stark basis, we see that a diagonal density matrix results in zero total current.²⁸ Thus, coherences are central to the transport process, even in the Wannier-Stark basis, see also Ref. 20. This conflicts with the common Wannier-Stark hopping picture. How do we reconcile these contradictions? The an-

swer is that the Wannier-Stark hopping model is derived from Eq. (2) by expressing, in a low-order approximation, the offdiagonal elements of the density matrix in terms of the diagonal elements.^{21,22,23} Under conditions where such an approximation is applicable the Wannier-Stark hopping model gives the same results as a full quantum transport model (see, e.g., Ref. 23 for superlattices), but it should be remembered that the Wannier-Stark hopping model uses populations which are in actual fact an approximation for the coherences.

Following the concepts of standard quantum optics, one is tempted to assume that coherences are created by the electric field and destroyed by scattering. However, the opposite is true in the quantum treatment of transport within the basis of Wannier-Stark states, which are eigenstates of \hat{H}_o including the electrostatic potential. Here coherences are induced by the scattering processes via the non-diagonal self-energies, which are crucial in a consistent quantum treatment.

VII. SUMMARY

We have shown that the entire current through QC structures is carried only by complex, quantum-mechanical wavefunctions as shown, e.g., in the upper panel of Fig. 3. This conclusion follows from two main results: (i) The scattering current J_{scatt} vanishes, which directly follows from $[\hat{H}_{\text{scatt}}, \hat{z}] = 0$, if the scattering potentials couple to the spatial coordinate of electron states. (ii) In the position basis, only the diagonal scattering matrix elements $V_{\alpha\alpha}$ are significant in determining the current J_o , and hence the entire current. Such matrix elements do not induce spatial translation of the electron state within the scattering transition. Thus, the principal scattering events which transfer momentum and/or dissipate energy in the transport process in quantum cascade structures occur only through spatially-local transitions which do not give rise to propagation of charge.

The locality of scattering transitions contrasts with the simple picture of electrons hopping between energy eigenstates due to scattering events, which is a common description in heterostructure systems. On the other hand, our point of view is analogous to bulk transport, where the scattering term in Boltzmann's equation is local in space, and the entire current is carried by Bloch states.

We thank R. Lake for helpful discussion. This work was supported by Deutsche Forschungsgemeinschaft and the Swedish Research Council.

* Electronic address: Andreas.Wacker@fysik.lu.se

¹ J. Faist, F. Capasso, D. L. Sivco, C. Sirtori, A. L. Hutchinson, and A. Y. Cho, *Science* **264**, 553 (1994).

² C. Gmachl, F. Capasso, D. L. Sivco, and A. Y. Cho,

Rep. Prog. Phys. **64**, 1533 (2001).

³ R. F. Kazarinov and R. A. Suris, *Sov. Phys. Semicond.* **6**, 120 (1972), [*Fiz. Tekh. Poluprov.* **6**, 148 (1972)].

⁴ K. Donovan, P. Harrison, and R. W. Kelsall, *J. Appl. Phys.*

- 89**, 3084 (2001).
- ⁵ R. C. Iotti and F. Rossi, Phys. Rev. Lett. **87**, 146603 (2001).
- ⁶ O. Bonno, J. Thobel, and F. Dessenne, J. Appl. Phys. **97**, 043702 (2005).
- ⁷ A. Mirčetić, D. Indjin, Z. Ikonjić, P. Harrison, V. Milanović, and R. W. Kelsall, J. Appl. Phys. **97**, 084506 (2005).
- ⁸ R. Tsu and G. Döhler, Phys. Rev. B **12**, 680 (1975).
- ⁹ F. Eickemeyer, K. Reimann, M. Woerner, T. Elsaesser, S. Barbieri, C. Sirtori, G. Strasser, T. Müller, R. Bratschkitsch, and K. Unterrainer, Phys. Rev. Lett. **89**, 047402 (2002).
- ¹⁰ M. Woerner, K. Reimann, and T. Elsaesser, J. Phys.: Condens. Matter **16**, R25 (2004).
- ¹¹ H. Callebaut and Q. Hu, J. Appl. Phys. **98**, 104505 (2005).
- ¹² N. W. Ashcroft and N. D. Mermin, *Solid State Physics* (Saunders College, Philadelphia, 1976).
- ¹³ S.-C. Lee and A. Wacker, Phys. Rev. B **66**, 245314 (2002).
- ¹⁴ C. Sirtori, P. Kruck, S. Barbieri, P. Collot, J. Nagle, M. Beck, J. Faist, and U. Oesterle, Appl. Phys. Lett. **73**, 3486 (1998).
- ¹⁵ B. S. Williams, H. Callebaut, S. Kumar, Q. Hu, and J. L. Reno, Appl. Phys. Lett. **82**, 1015 (2003).
- ¹⁶ R. K. Lake and R. R. Pandey, *Nonequilibrium Green functions in electronic device modeling*, preprint.
- ¹⁷ R. Lake, G. Klimeck, R. C. Bowen, and D. Jovanovic, J. Appl. Phys. **81**, 7845 (1997).
- ¹⁸ G. D. Mahan, Phys. Rep. **145**, 251 (1987).
- ¹⁹ S. Zeuner, B. J. Keay, S. J. Allen, K. D. Maranowski, A. C. Gossard, U. Bhattacharya, and M. J. W. Rodwell, Phys. Rev. B **53**, 1717 (1996).
- ²⁰ R. C. Iotti, E. Ciancio, and F. Rossi, Phys. Rev. B **72**, 125347 (2005).
- ²¹ D. Calecki, J. F. Palmier, and A. Chomette, J. Phys. C: Solid State Phys. **17**, 5017 (1984).
- ²² Y. Lyanda-Geller and J.-P. Leburton, Semicond. Sci. Technol. **10**, 1463 (1995).
- ²³ A. Wacker, Phys. Rep. **357**, 1 (2002).
- ²⁴ F. Banit, S.-C. Lee, A. Knorr, and A. Wacker, Appl. Phys. Lett. **86**, 41108 (2005).
- ²⁵ For Σ^{ret} and self-energies for other scattering processes, see Ref. 13. Impurity scattering is treated microscopically as in Ref. 24. We only treat electron-electron scattering in a mean field approximation, but it has been shown that for intersubband transport, electron-impurity scattering usually dominates over electron-electron scattering, see Callebaut, Kumar, Williams, Hu, and Reno, Appl. Phys. Lett. **84**, 645 (2004).
- ²⁶ We use an iterative scheme based on the Broyden method, V. Eyert, J. Comp. Physics **124**, 271 (1996).
- ²⁷ As a further check on the calculation, current continuity requires that the integration of Eq. (3) over energy should result in $J_o(z) = \int dE J_o(z, E) = \text{a constant}$. Numerically, we observe a spatial variation due to the limited number of basis states used in the calculation. Increasing the number of basis states to 8 Wannier states per period (also used in Fig. 3) reduces this variation to $< 10\%$.
- ²⁸ This can also be seen in Eq. (4) of Ref. 21 or Eq. (9) of Ref. 22.